JACS
JOURNAL OF THE AMERICAN CHEMICAL SOCIETY

ARTICLE

pubs.acs.org/JACS

Interfacial Engineering of Organic Nanofibril Heterojunctions into Highly Photoconductive Materials

Yanke Che, Helin Huang, Miao Xu, Chengyi Zhang, Benjamin R. Bunes, Xiaomei Yang, and Ling Zang*

Department of Materials Science and Engineering, University of Utah, Salt Lake City, Utah 84108, United States

Supporting Information

ABSTRACT: Photoconductive organic materials have gained increasing interest in various optoelectronics, such as sensors, photodetectors, and photovoltaics. However, the availability of such materials is very limited due to their intrinsic low charge carrier density and mobility. Here, we present a simple approach based on nanofibril heterojunction to achieve high photoconductivity with fast photoresponse, that is, interfacial engineering of electron donor (D) coating onto acceptor (A) nanofibers via optimization of hydrophobic interaction between long alkyl side-chains. Such nanofibril heterojunctions possess two prominent features that are critical for efficient photocurrent generation: the nanofibers both create a large D/A interface for increased charge separation and act as long-range transport pathways for photogenerated charge carriers toward the electrodes, and the alkyl groups employed not only enable effective surface adsorption of D molecules on the nanofibers for effective electron-transfer communication, but also spatially separate the photogenerated charge carriers to prevent their recombination. The reported approach represents a simple, adaptable method that allows for the development and optimization of photoconductive organic materials.

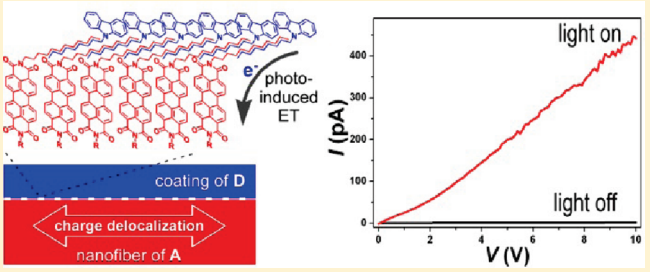

INTRODUCTION

Photoconductive organic materials have attracted increasing interest due to their potential applications in photodetectors,[1−4] sensors,[5−7] and photovoltaics.[8−10] However, the available organic materials are very limited due to their intrinsic low charge carrier density and mobility. Although bulk heterojunctions of electron donors (D) and acceptors (A) allow for generation of photocurrent, the formation of charge-transfer complex and the lack of long-range charge transport pathway result in loss of the photogenerated charge carriers through recombination.[3,11] One-dimensional organic nanostructures assembled via $\pi-\pi$ interactions present promising candidates for highly photoconductive materials due to their enhanced charge carrier mobility.[12−16] However, only a few examples of photoconductive one-dimensional nanostructures have been reported,[3,5,8,17−19] and most of them are focused on the covalently linked D−A molecules.[3,5,8,17] Obvious disadvantages of these systems include complicated molecular design and synthesis, and challenges in optimization of the intermolecular assembly so as to avoid charge carrier recombination, making them impractical in large-scale applications. Therefore, it is highly demanding to develop simple and general methods to fabricate photoconductive organic materials. Here, we present a simple approach based on nanofibril heterojunctions (Scheme1) to achieve high photoconductivity and fast photoresponse with a large on/off ratio above 10^4 for organic semiconductor materials, that is, interfacial engineering of D molecule coating onto A nanofibers via optimization of the hydrophobic interaction between long alkyl side-chains. We find that the hydrophobic interaction between alkyl side-chains enables effective adsorption of D molecules onto A nanofibers, for which the surface binding of D can be further strengthened by increasing the numbers of alkyl chains in D molecules. The resulting interface via alkyl interdigitation was demonstrated to be capable of tuning both the photoinduced electron transfer from D to A and the charge recombination, thus providing optimization of the photoconductive performance of the nanofibril heterojunctions thus fabricated. We anticipate that this simple approach to fabrication of highly photoconductive organic materials will lead to more options for the new materials design and performance improvement and optimization.

RESULTS AND DISCUSSION

Fabrication of Nanofibril Heterojunctions. Figure 1 shows the nanofibers assembled from A-1 molecules (Scheme 1) using a previously reported method.[20,21] These nanofibers are several micrometers long and tens of nanometers wide. Such thin nanofibers possess large surface area allowing for surface adsorption of D molecules to produce wide D/A interface, which in turn leads to efficient dissociation of excitons into separated charge carriers through interfacial electron transfer as illustrated in Scheme 1. Because the strong $\pi-\pi$ stacking interaction between the A molecules (the perylene planes) results in effective π-electron delocalization, that is, enhanced electron migration along the long axis of nanofiber,[5,11−13]

Received: October 18, 2010
Published: December 23, 2010

Scheme 1. Schematic Illustration of Nanofibril Heterojunctions Composed of Electron Donor (D)-Coated Nanofibers That Function as Electron Acceptor (A)[a]

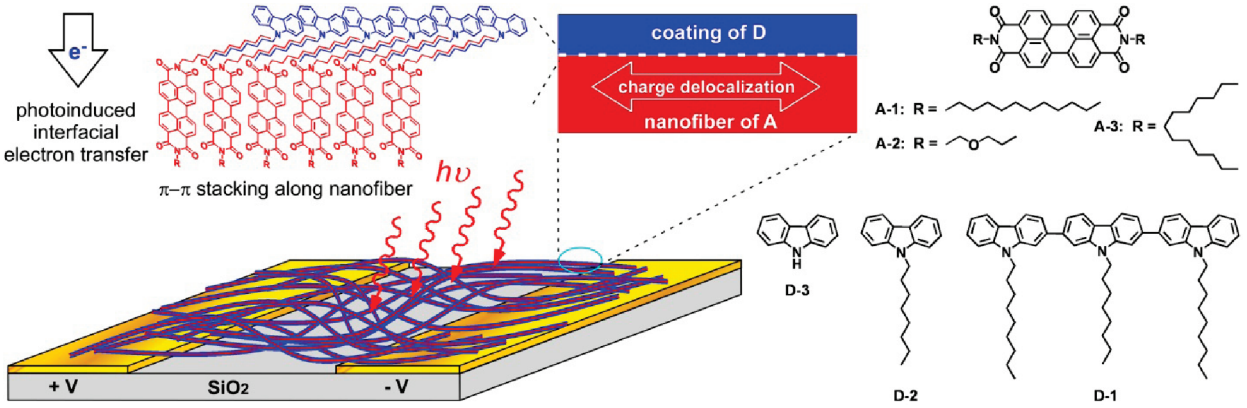

[a] The π-stacking along the long axis of nanofiber is conducive to enhancement of charge transport due to the intermolecular π-electron delocalization. The photoinduced electron transfer in this case is more of an interfacial process, where the interdigitated alkyl chains can inhibit the back electron transfer to a certain extent depending on the length of the alkyl chains. Molecular structures of the three electron acceptors (A-1, A-2, A-3) and three electron donors (D-1, D-2, D-3) are shown in the right panel.

the separated charge carriers can be collected at two electrodes upon application of an electrical bias.

With the nanofiber as efficient charge conduit, the next critical criterion for achieving high photocurrent with the fibril heterojunctions is to prevent the back electron transfer (i.e., the charge recombination between the photogenerated electron and hole), which indeed represents one of the major causes for charge loss in bulk heterojunction materials, for example, C60/polymers.[10] To this end, we designed and synthesized D-1 molecule (Scheme 1), which possesses three long alkyl chains and is expected to strongly bind to the surface of nanofibers that are self-assembled from the A molecules (e.g., A-1) with similar linear alkyl side-chains. Meanwhile, the space separation caused by the interdigitated alkyl chains would inhibit the charge recombination between the photogenerated anionic and cationic radicals. The nanofibril heterojunctions were fabricated simply by drop-casting an ethanol solution of D-1 onto the A-1 nanofibers deposited on silica substrate. Interestingly, as evidenced by SEM and AFM images (Figure 1b, d, f), most D-1 molecules were bound to the nanofibers upon vaporization of the solvent, and no apparent D-1 materials similar to the film morphology formed by direct drop-casting of the ethanol solution of D-1 onto the same substrate (Figure S1) were observed between the nanofibers. A close examination of AFM images clearly shows D-1 molecules were mostly adsorbed on the surface of A-1 nanofibers (Figure 1e and f). The spontaneous adsorption and concentration of D-1 molecules onto A-1 nanofibers is likely driven by the hydrophobic interaction between the alkyl side-chains as mentioned above. In comparison, the highly hydrophilic surface of silica is not favored for strong binding with the D-1 molecules. Indeed, drop-casting of the same D-1 solution onto silica led to formation of broken films consisting of thin flakes and particulate aggregates (Figure S1), mainly caused by the surface dewetting. The observed one-step coating of D over A nanostructured materials provides a simple, clean method for construction of large area D/A heterojunctions with wide interface.

Apparently, the nanofibril heterojunctions thus fabricated prevent the formation of a charge-transfer complex of **D**−A as the A-1 nanofibers were preassembled without the interference of D molecules, and the fibril materials are robust against the drop-casting solvent (i.e., A-1 molecules are insoluble in ethanol). In contrast, formation of D−A charge-transfer complex is usually difficult to avoid in bulk heterojunction materials,[11,22,23] where the intracomplex charge recombination dominates the loss of charge carriers. The nanofibril heterojunction system as presented in Scheme 1 also demonstrates practical advantages in comparison to the materials fabricated from covalently linked D−A molecules, which often require much more complicated molecular design and synthesis, and thus offer limited choices for the structural optimization of D and A molecules.

Photoconductivity of the Nanofibril Heterojunctions. As shown in Figure 2a, high photoconductivity was observed for the nanofibril heterojunctions as presented in Figure 1, whereas negligible photocurrent was measured for the pristine A-1 nanofibers or pure D-1 film (Figure S2). The photocurrent also increased with the amount of D-1 added at the initial stage until a saturated region is reached at a molecular molar ratio of A-1 to D-1 of about 2. At this molar composition, the nanofibril heterojunction demonstrated a photocurrent on/off ratio above 10^4 when measured on a micro−electrode pair (90 μm wide and 5 μm gap) under a bias of 10 V (Figure S3). Given that the average irradiation light is 550 nm, the quantum efficiency of the photocurrent generation can be estimated as ca. 8% under an electrical field of 2 V/μm by using the same calculation method as previously reported.[24,25] The photocurrent was found also switching promptly with light on and off (Figure 3b), indicating a response time of only ca. 200 ms (Figure S6). The fast photoresponse as observed, together with the high on/off ratio, makes the nanofibril heterojunctions attractive for application in optoelectronic devices.

Consistent with the high photocurrent generation, the fluorescence of A-1 nanofibers was also found to be effectively quenched upon adsorption of D-1 molecules (Figure 2c). Because the absorption edge of D-1 is far below 400 nm, the observed fluorescence quenching of nanofibers is unlikely due to energy transfer, but rather solely due to the interfacial electron transfer from D to the photoexcited A as illustrated in Scheme 1. Such photoinduced electron transfer is highly favored with a driving force of 0.95 eV (Figure S4). As such, fluorescence quenching in such system denotes the forward electron transfer from D to A-1 nanofibers upon irradiation. Interestingly, ca. 13% molar fraction of D-1 quenched ca. 55% of the fluorescence of A-1 nanofibers. This amplified fluorescence

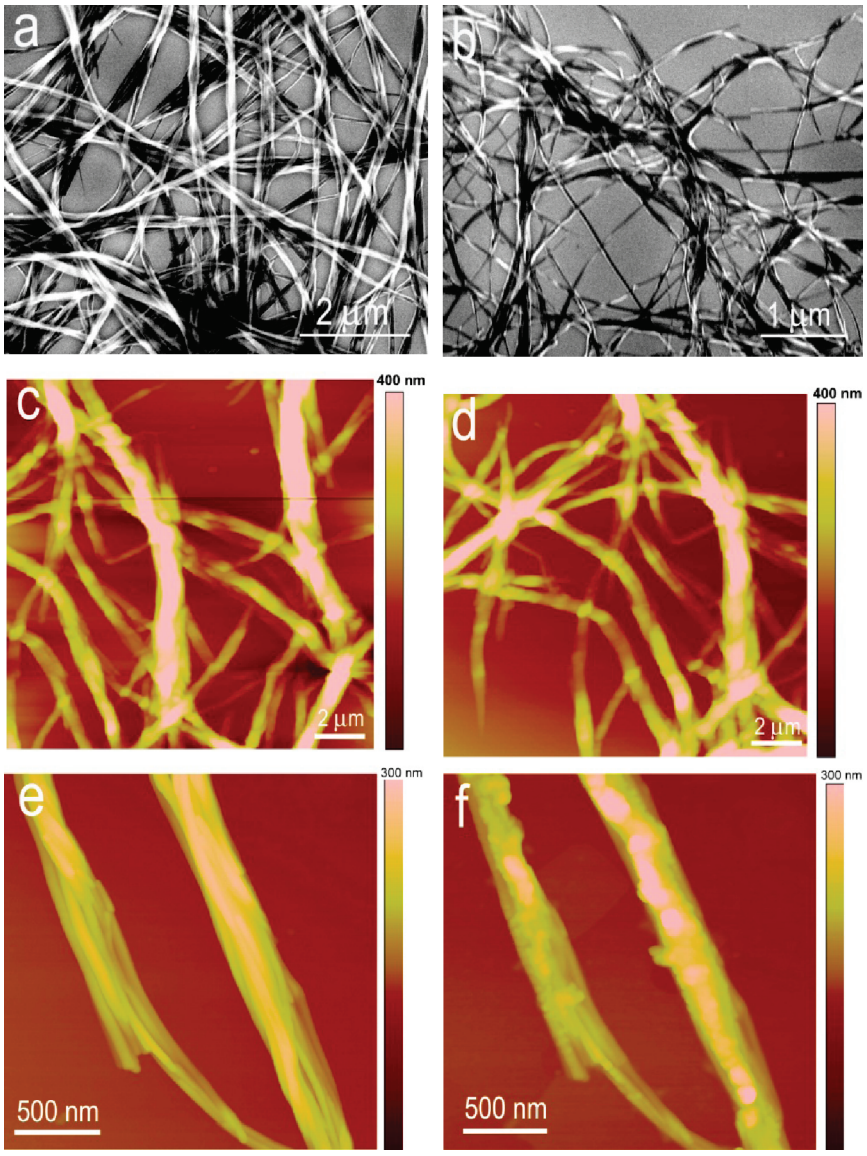

Figure 1. A-1 nanofibers before (a,c,e) and after (b,d,f) being coated with D-1 molecules. (a) SEM image of pristine nanofibers deposited on the silica. (b) SEM image of the nanofibers (7.5 nmol of A-1 molecules) after being coated with D-1 by drop-casting an ethanol solution of D-1 (4 nmol) onto the fibril network as shown in (a), where almost no separate phase of D-1 was formed between the nanofibers. (c and e) AFM image of the same A-1 nanofibers as shown in (a). (d and f) AFM image of the D-1-coated nanofibers as shown in (b). AFM imaging clearly shows the surface deposition of D-1, as envisioned by the increased *z*-height of the line scanning profile. However, no apparent thickness increase was found for the spare area between the nanofibers, indicating effective concentration of D-1 onto the nanofibers.

quenching implies the existence of exciton diffusion within A-1 nanofibers, as previously indicated in other nanostructured systems.[26] Because the nanofibril heterojunctions are formed by the adsorption of D-1 molecules via the hydrophobic interaction between alkyl groups, it is expected that the adsorption and desorption of D-1 can be readily switched, making the photoconductivity reversible. Indeed, the reversible photoconductivity was achieved simply by washing away the D-1 molecules with ethanol and redeposition of its ethanol solution onto the nanofibers (Figure S5). Thinking of the potential degeneration of the photoconductivity of organic materials caused by the photooxidation, the easy regeneration of photoconductivity is attractive for practical applications.

Interfacial Influence on the Photoconductivity. Although efficient photoinduced electron transfer was previously observed for the perylene diimide-based supramolecular D/A systems,[27−29] no significant photoconductivity has yet been achieved with these materials. To gain an insight into the origin of the high photoconductivity as achieved in Figure 2, we investigated various D and A molecules bearing different side groups (Scheme 1), which formulate the heterojunction interface and affect greatly the D/A interaction. As shown in Figure 3, all three D molecules demonstrated efficient fluorescence quenching of the A-1 nanofibers when coated onto the surface, indicating the occurrence of photoinduced electron transfer from D to A upon photoillumination. However, significant photocurrent was only obtained with D-1 and D-2 molecules bearing long alkyl groups, whereas D-3 generated negligible current under the same conditions. This result implies that introduction of alkyl groups can effectively prevent the recombination of photogenerated charge carriers through spatial separation. Such spatial effect on the prevention of charge carrier

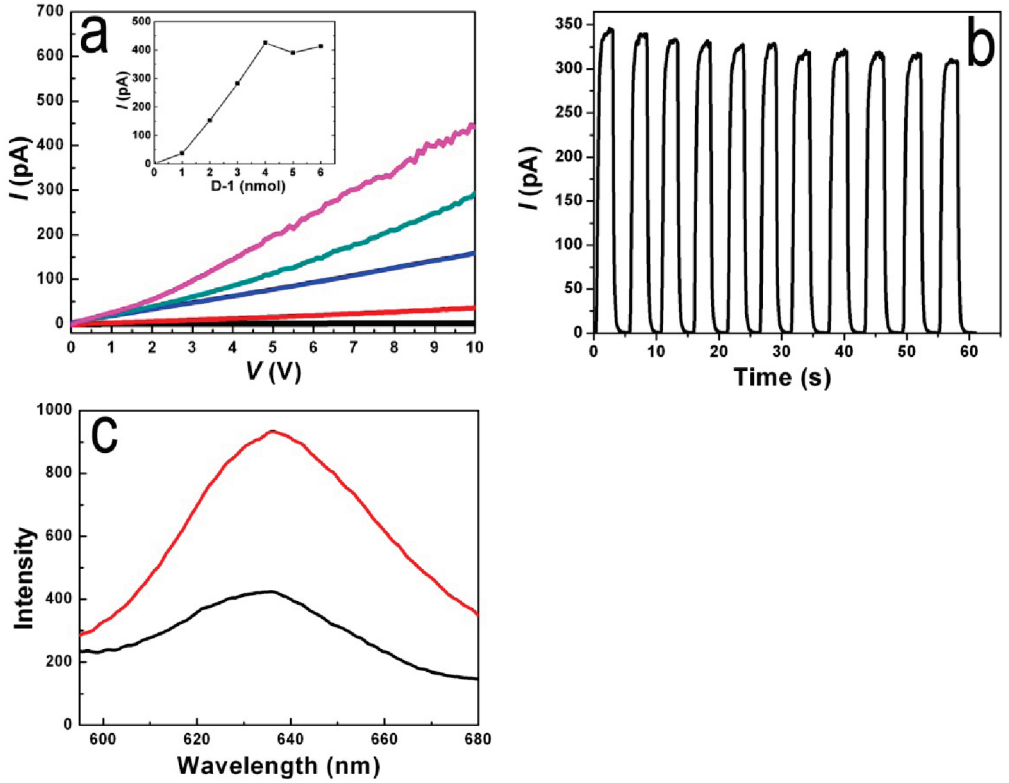

Figure 2. (a) $I-V$ curves measured over the A-1 nanofibers with increasing deposition of D-1 through drop-casting of the ethanol solution (0.1 mM) (black:, pristine nanofibers containing 7.5 nmol of A-1; red, blue, green, magenta, deposition of 1, 2, 3, 4 nmol of D-1, respectively); white light irradiation was set at a power density of 0.17 mW/mm^2. (b) Photocurrent measured at 10 V of bias in response to turning on and off the white light irradiation (0.17 mW/mm^2). (c) Fluorescence spectra of A-1 nanofibers (containing 7.5 nmol of A-1) measured before (red) and after (black) deposition of 1 nmol of D-1. Electrode pairs used: 5 μm in gap, 14 μm in width. All measurements were carried out under ambient condition.

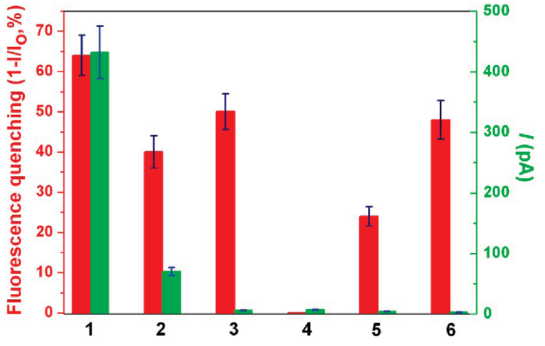

Figure 3. Comparison of optical and electrical performance between various D/A heterojunctions. The red and green columns denote fluorescence quenching and photocurrent measurement, respectively. (1) Nanofibers of A-1 (7.5 nmol) deposited with 4 nmol of D-1; (2) nanofibers of A-1 (7.5 nmol) deposited with 60 nmol of D-2; (3) nanofibers of A-1 (7.5 nmol) deposited with 20 nmol of D-3; (4) nanofibers of A-2 (7.5 nmol) deposited with 15 nmol of D-1; (5) film of A-3 (10 nmol) deposited with 20 nmol of D-1; and (6) film of A-3 (10 nmol) deposited with 60 nmol of D-3. Electrode configuration and measurement conditions are the same as employed in Figure 2.

recombination is analogous to that observed in the one-dimensional nanostructures composed of covalently linked D−A molecules.[3,5] Here, it can be speculated that the spatial segregation can be optimized toward the photocurrent generation by altering the length of alkyl chains, and the work along this line is in progress.

As compared to D-2, D-1 exhibited about 6 times higher photocurrent despite 15 times molar excess of D-2 was used. This observation can be interpreted by the fact that the three alkyl chains borne with D-1 make it binding to the nanofibers much stronger to allow electron-transfer communication more efficiently. The stronger interfacial binding is indeed supported by the higher fluorescence quenching efficiency as observed for even less D-1 used (Figure 3). To further study the influence of side groups on the interfacial D/A interaction, we fabricated nanofibers from A-2 molecules, which possess the same π-scaffold as A-1, but bear short, more hydrophilic side-chains, which are not compatible with D-1 bearing the hydrophobic side-chains. This should result in a separated interface between D-1 phase and A-2 fibers, which thus inhibit the electron-transfer communication at the D/A interface. Indeed, the heterojunction system fabricated from A-2 fibers and D-1 molecules exhibited neither fluorescence quenching nor photocurrent generation (Figure 3). This negative observation further supports the importance of alkyl groups to photocurrent generation.

To verify the critical effect of one-dimensional $\pi-\pi$ stacking as envisioned in the nanofibril structure on the photocurrent generation, we investigated another heterojunction system fabricated by adsorption of D molecules on the film of A-3. Because of the steric hindrance of the branched side groups of A-3, it is impossible to fabricate highly organized materials from this molecule, particularly with $\pi-\pi$ stacking along one dimension.[20] Although efficient electron transfer can take place at the D/A interface upon irradiation, as evidenced by the significant fluorescence quenching of the film

dx.doi.org/10.1021/ja109396g |J. Am. Chem. Soc. 2011, 133, 1087–1091

upon coating with D-3 and D-1 (Figure 3), negligible photocurrent was observed for these film-based heterojunctions, likely due to the lack of effective charge transport pathways within the film. This result indicates that the A-1 nanofibers as employed indeed play a critical role enabling rapid transport of the charge carriers toward the electrodes.

In conclusion, highly photoconductive organic nanofibril heterojunctions have been fabricated through simple interfacial engineering of the hydrophobic interaction between alkyl side-chains. Such nanofibril heterojunctions possess two prominent features that are critical for efficient photocurrent generation: one is that the nanofibers both create wide D/A interface for increased charge separation and act as long-range transport pathway for photogenerated charge carriers toward the electrodes; and the other is that the alkyl groups employed not only enable effective surface adsorption of D molecules on the nanofibers for effective electron-transfer communication, but also spatially separate the photogenerated charge carriers to prevent their recombination. The reported approach represents a simple, adaptable method allowing for the development and optimization of photoconductive supramolecular organic materials.

■ ASSOCIATED CONTENT

Supporting Information. DFT calculations, AFM image, and more optical/electrical measurements. This material is available free of charge via the Internet at http://pubs.acs.org.

■ AUTHOR INFORMATION

Corresponding Author
lzang@eng.utah.edu

■ ACKNOWLEDGMENT

This work was supported by the NSF (CAREER CHE 0641353, CBET 730667), the DHS (2009-ST-108-LR0005), and the USTAR Program.

■ REFERENCES

(1) Gong, X.; Tong, M.; Xia, Y.; Cai, W.; Moon, J. S.; Cao, Y.; Yu, G.; Shieh, C.-L.; Nilsson, B.; Heeger, A. J. *Science* **2009,** *325*, 1665–1667.
(2) Konstantatos, G.; Sargent, E. H. *Nat. Nanotechnol.* **2010,** *5*, 391–400.
(3) Yamamoto, Y.; Fukushima, T.; Suna, Y.; Ishii, N.; Saeki, A.; Seki, S.; Tagawa, S.; Taniguchi, M.; Kawai, T.; Aida, T. *Science* **2006,** *314*, 1761–1764.
(4) Zhu, H.; Li, T.; Zhang, Y.; Dong, H.; Song, J.; Zhao, H.; Wei, Z.; Xu, W.; Hu, W.; Bo, Z. *Adv. Mater.* **2010,** *22*, 1645–1648.
(5) Che, Y.; Yang, X.; Liu, G.; Yu, C.; Ji, H.; Zuo, J.; Zhao, J.; Zang, L. *J. Am. Chem. Soc.* **2010,** *132*, 5743–5750.
(6) Che, Y.; Yang, X.; Zhang, Z.; Zuo, J.; Moore, J. S.; Zang, L. *Chem. Commun.* **2010,** *46*, 4127–4129.
(7) Zhang, X.; Jie, J.; Zhang, W.; Zhang, C.; Luo, L.; He, Z.; Zhang, X.; Zhang, W.; Lee, C.; Lee, S. *Adv. Mater.* **2008,** *20*, 2427–2432.
(8) Yamamoto, Y.; Zhang, G.; Jin, W.; Fukushima, T.; Ishii, N.; Saeki, A.; Seki, S.; Tagawa, S.; Minari, T.; Tsukagoshi, K.; Aida, T. *Proc. Natl. Acad. Sci. U.S.A.* **2009,** *106*, 21051–21056; S21051/1−S21051/12.
(9) Charvet, R.; Acharya, S.; Hill, J. P.; Akada, M.; Liao, M.; Seki, S.; Honsho, Y.; Saeki, A.; Ariga, K. *J. Am. Chem. Soc.* **2009,** *131*, 18030–18031.
(10) Clarke, T. M.; Durrant, J. R. *Chem. Rev.* **2010,** *110*, 6736–6767.
(11) Neuteboom, E. E.; Meskers, S. C. J.; Van Hal, P. A.; Van Duren, J. K. J.; Meijer, E. W.; Janssen, R. A. J.; Dupin, H.; Pourtois, G.; Cornil, J.; Lazzaroni, R.; Bredas, J.-L.; Beljonne, D. *J. Am. Chem. Soc.* **2003,** *125*, 8625–8638.
(12) Coropceanu, V.; Cornil, J.; Da Silva Filho, D. A.; Olivier, Y.; Silbey, R.; Bredas, J.-L. *Chem. Rev.* **2007,** *107*, 926–952.
(13) Che, Y.; Datar, A.; Yang, X.; Naddo, T.; Zhao, J.; Zang, L. *J. Am. Chem. Soc.* **2007,** *129*, 6354–6355.
(14) Sofos, M.; Goldberger, J.; Stone, D. A.; Allen, J. E.; Ma, Q.; Herman, D. J.; Tsai, W.-W.; Lauhon, L. J.; Stupp, S. I. *Nat. Mater.* **2009,** *8*, 68–75.
(15) Ruiz Delgado, M. C.; Kim, E.-G.; da Silva Filho, D. A.; Bredas, J.-L. *J. Am. Chem. Soc.* **2010,** *132*, 3375–3387.
(16) Messmore, B. W.; Hulvat, J. F.; Sone, E. D.; Stupp, S. I. *J. Am. Chem. Soc.* **2004,** *126*, 14452.
(17) Hizume, Y.; Tashiro, K.; Charvet, R.; Yamamoto, Y.; Saeki, A.; Seki, S.; Aida, T. *J. Am. Chem. Soc.* **2010,** *132*, 6628–6629.
(18) Jiang, L.; Fu, Y.; Li, H.; Hu, W. *J. Am. Chem. Soc.* **2008,** *130*, 3937.
(19) Luo, J.; Yan, Q.; Zhou, Y.; Li, T.; Zhu, N.; Bai, C.; Cao, Y.; Wang, J.; Pei, J.; Zhao, D. *Chem. Commun.* **2010,** *46*, 5725–5727.
(20) Balakrishnan, K.; Datar, A.; Naddo, T.; Huang, J.; Oitker, R.; Yen, M.; Zhao, J.; Zang, L. *J. Am. Chem. Soc.* **2006,** *128*, 7390–7398.
(21) Zang, L.; Che, Y.; Moore, J. S. *Acc. Chem. Res.* **2008,** *41*, 1596–1608.
(22) Pisula, W.; Kastler, M.; Wasserfallen, D.; Robertson Joseph, W. F.; Nolde, F.; Kohl, C.; Mullen, K. *Angew. Chem., Int. Ed.* **2006,** *45*, 819–23.
(23) Percec, V.; Glodde, M.; Bera, T. k.; Miura, Y.; Shiyanovsaya, I.; Singer, K. D.; Balagurusamy, V. S. K.; Helney, P. A.; Schnell, I.; Rapp, A.; Spiess, H. W.; Hudson, S. D.; Duan, H. *Nature* **2002,** *417*, 384–387.
(24) Schwab, A. D.; Smith, D. E.; Bond-Watts, B.; Johnston, D. E.; Hone, J.; Johnson, A. T.; dePaula, J. C.; Smith, W. F. *Nano Lett.* **2004,** *4*, 1261–1265.
(25) O'Brien, G. A.; Quinn, A. J.; Tanner, D. A.; Redmond, G. *Adv. Mater.* **2006,** *18*, 2379–2383.
(26) Yamamoto, Y.; Fukushima, T.; Saeki, A.; Seki, S.; Tagawa, S.; Ishii, N.; Aida, T. *J. Am. Chem. Soc.* **2007,** *129*, 9276–9277.
(27) Wurthner, F.; Chen, Z.; Hoeben, F. J. M.; Osswald, P.; You, C. C.; Jonkheijm, P.; Herrikhuyzen, J. v.; Schenning, A. P. H. J.; vanderSchoot, P. P. A. M.; Meijer, E. W.; Beckers, E. H. A.; Meskers, S. C. J.; Janssen, R. A. J. *J. Am. Chem. Soc.* **2004,** *126*, 10611–10618.
(28) Van Herrikhuyzen, J.; Syamakumari, A.; Schenning, A. P. H. J.; Meijer, E. W. *J. Am. Chem. Soc.* **2004,** *126*, 10021–10027.
(29) Beckers Edwin, H. A.; Meskers Stefan, C. J.; Schenning Albertus, P. H. J.; Chen, Z.; Wurthner, F.; Marsal, P.; Beljonne, D.; Cornil, J.; Janssen Rene, A. J. *J. Am. Chem. Soc.* **2006,** *128*, 649–57.